Study of Winglets Performance for Small Hydrofoil Craft Using Computational Fluid Dynamics

Wira Setiawan[1],[*], Muhammad Irsyaduddin Romadhoni[1], Andi Mursid Nugraha Arifuddin[1], M. Uswah Pawara[1], Suardi[1]

[1] Departement of Naval Architecture, Institut Teknologi Kalimantan, Balikpapan, 76127, East Kalimantan, Indonesia

ARTICLE INFO	ABSTRACT
    	A hydrofoil ship excels in high-speed travel with fuel efficiency due to reduced resistance. However, utilizing the submerged surface results in turbulent flow from fluid interactions on the hydrofoil's surfaces. The solution involves appropriately affixing winglets, similar to those on airplane wings. This study investigates various winglet designs for optimal selection; whilst their influence on vortices through computational fluid dynamics (CFD). The hydrofoil-winglet flow pattern, lift, and drag are then assessed through parametric winglet variation. The winglet-less hydrofoil (W0) generates high lift but substantial drag, leading to an unfavourable L/D ratio. Absence of a winglet at the hydrofoil tip causes increased pressure gradient, inducing vortex drag. In contrast, the W1 model, equipped with an enclosed winglet, outperforms in maintaining pressure-side flow, yielding the highest L/D ratio. Attaching winglets to the hydrofoil's edges could potentially reduce surface vortices. In general, these findings contribute to the advancement of efficient and innovative maritime transportation solutions.

1. Introduction

The Hydrofoil vessel, a remarkable high-speed planing-hull ship, employs hydrofoils interconnected by struts beneath its hull, generating lift that elevates the vessel above water level. This reduces draft, minimizes wetted surface area, and decreases resistance, contributing to higher speeds [1]. The lift coefficient, influenced by the intricate hydrofoil shape, peaks just before the stall condition, while drag is affected by the drag coefficient (cd), shaping the vessel's aerodynamic performance.

For small hydrofoil craft, tailored for routes like Balikpapan-Penajam Paser Utara, the NACA 64 (1) 212 foil at a 20° attack angle excels in lift force and cl/cd ratio, lifting the hull above water at 30 knots, significantly reducing resistance [2]. This triggers events that intricately affect lift and drag coefficients, explored by Suryadi *et al.,* [3] and Ni *et al.,* [4], highlighting the dynamic forces governing hydrofoil performance.

---

[*] *Corresponding author.*
E-mail address: wira@itk.ac.id

Hydrofoils submerged below water introduce turbulence due to fluid interaction on suction and pressure sides. Winglets, akin to aircraft wings, counter this by connecting vertical appendages to horizontal hydrofoils [5,6]; reducing drag and vortices, enhancing fuel efficiency [7-9]. Winglet design parameters like can't angles reduce drag [10], while can't and sweep angles enhance the lift-to-drag (L/D) ratio [11]. The hydrofoil's taper, aspect ratio, and winglet shape intricately influence lift and drag coefficients [12]. Numerical simulations explore vortex behavior around elliptical hydrofoils [13,14]; experimentally explore dihedral angles to mitigate tip vortex cavitation.

This study presents winglet selections for refining small hydrofoil craft design using computational fluid dynamics (CFD) (Figure 1). Analysis of varied winglet geometrical parameters assesses forces, lift-to-drag ratios, and hydrofoil vortices. The solution involves attaching winglets, akin to aircraft wings. The investigation explores diverse winglet designs, evaluating their impact on vortices. Subsequent exploration systematically examines hydrofoil-winglet flow patterns, lift, and drag, offering insights into efficient maritime transportation solutions.

Fig. 1. Hydrofoil craft equipped with winglet

2. Theoretical Background

The basic equation of lift and drag force obtained from the performance of hydrofoil depends on the fluid density, ship velocity, plan area and the lift and drag coefficients (Eq. (1) and Eq. (2)).

$$F_l = \frac{1}{2} \rho \, v^2 \, A_p C_l \tag{1}$$

$$F_d = \frac{1}{2} \rho \, v^2 \, A_p C_d \tag{2}$$

Computational fluid dynamics software solves fluid dynamics behaviour using the Navier-Stokes equation, which is based on the conservation of mass equation (Eq. (3)).

$$\frac{\delta \rho}{\delta t} + \frac{\delta \rho u_i}{\delta x_i} = 0 \tag{3}$$

The Navier-Stokes equations (Eq. (4)) control momentum conservation, forces, acceleration, and fluid behaviour. These equations are solved numerically using methods such as finite volume or finite element to calculate fluid velocity and pressure fields.

$$\frac{\delta u_i}{\delta t} + u_j \frac{\delta u_t}{\delta x_j} = f_i - \left(\frac{1}{\rho} \frac{\delta_p}{\delta x_i}\right) + \left(\frac{1}{\rho} \frac{\delta \tau_y}{\delta x_j}\right) \tag{4}$$

where u_i is the velocity vector, f_i are the external body forces per unit mass, ρ is the density, p is the pressure and τ_y represents the viscous stress tensor.

3. Simulation Condition

This section covers essential simulation conditions for hydrofoil winglet analysis, including the variation of type and dimensions, the computational domain, and mesh generation.

3.1 Winglet Geometry

Due to the fact that the winglet is a part of the hydrofoil, the shape of the hydrofoil will affect the design of the winglet. Based on the NACA foil, common geometric terminology that appears in various model foils includes chord length, upper and lower surfaces, maximum thickness, and the radius of the leading and trailing edges, as shown in Figure 2 below.
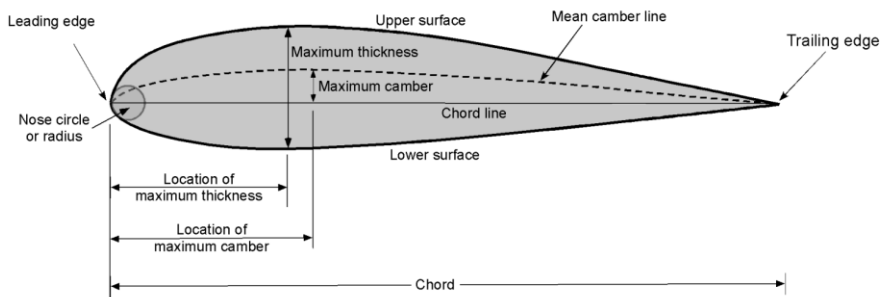

Fig. 2. Geometry Parameters of Airfoil [15]

Furthermore, winglets that are mounted on the end of the hydrofoil have several parameters such as the cant angle (β), sweep angle at the trailing edge winglet (ψ), winglet span (Sw), length of hydrofoil chord (c), tip chord length (Cwt), and root chord length (Cwr), as depicted in Figure 3 below.
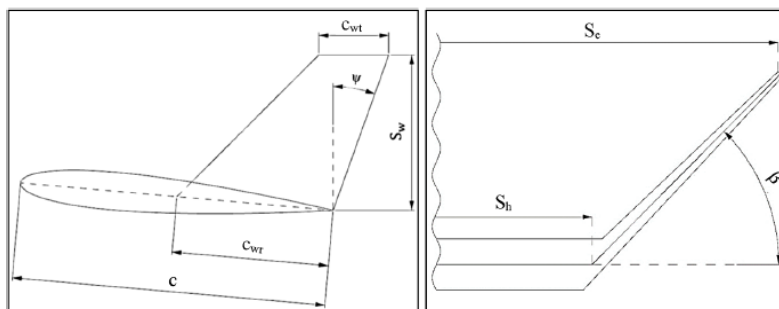

Fig. 3. The geometric parameters of the hydrofoil and winglets [6]

Table 1
Results of drag force analysis

Type	CCR	SCR	Direction	Ψ (°)	β (°)
W0	0	0	-	-	-
W1	1	0,5	Upward	0	90
W2	0,75	0,5	Upward	0	90
W3	0,5	0,5	Upward	0	90

This study varies four types of winglets referred from the research conducted by Çetinkaya and Oral Ünal [6], with an alteration in the size of the hydrofoil winglet to fit the vessel dimension. The winglets differ from the parameters of the ratio of the cwr to c (CCR) and the ratio of the Sw to c (SCR). Besides that, the winglet direction, ψ, and β are also determined as shown in table 1. The basic shape of the hydrofoil winglet is the NACA 64 (1) 212 airfoil with an attack angle of 20°

3.2 Hydrofoil Winglet Design

Based on the winglet geometry parameters in Table 1, the reference design of the hydrofoil winglet is the W0 type, as shown in Figure 4 below. It illustrates that the chord length of the foil (c) is 100 mm, and the span length is 1200 mm, without being equipped with winglets at the end (bare hydrofoil). The chord length of the foil, the span, and the angle of attack remain constant for the other variations of the winglet.
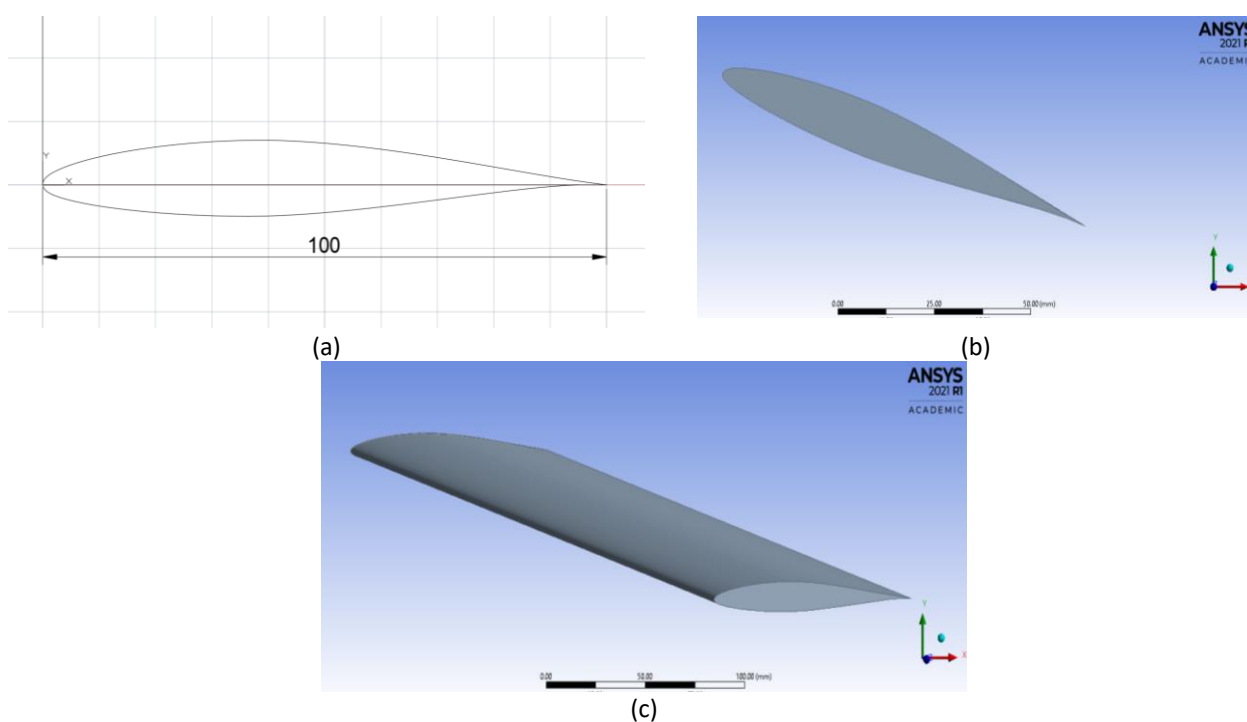

(a)

(b)

(c)

Fig. 4. Hydrofoil NACA 64(1) 212 (a), Set-up angle of attack 20˚ (b), and isometric view of W0 (c)

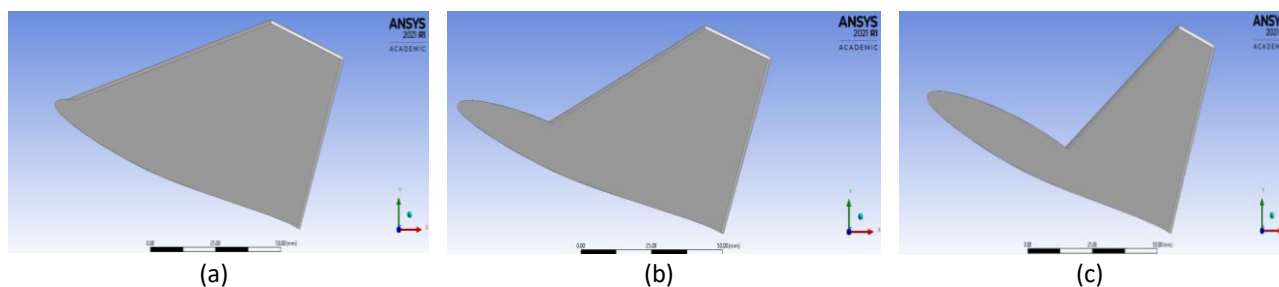(a)   (b)   (c)

Fig. 5. Side view of winglet W1 (a), W2 (b) and W3 (c)

Figure 5(a) depicts the winglet W1 with a root chord length (Cwr) of 100 mm, a span length (Cw) of 50 mm, and a tip chord length (Cwt) of 30 mm. The thickness of all the winglets is 10 mm. In addition, Figure 5(b) shows winglet W2 with Cwr = 75 mm, Cw = 50 mm, and Cwt =25 mm. The last

winglet, W3, shown in Figure 5(c), has Cwr = 50 mm, Cw = 50 mm, and Cwt = 17.5 mm. The isometric views of winglets W1, W2, and W3 are illustrated in Figure 6.
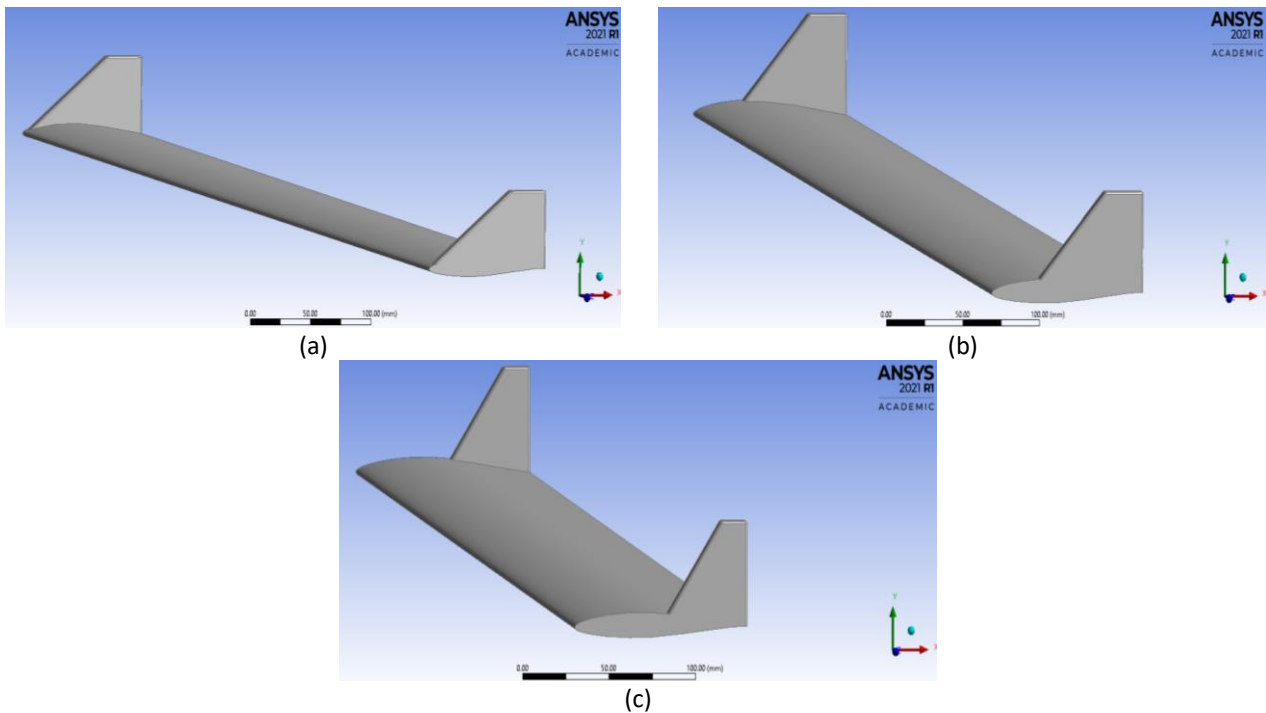

(a)

(b)

(c)

Fig. 6. Isometric view of winglet W1 (a), W2 (b) and W3 (c)

To obtain the performance of the hydrofoil winglets, the setup of the ANSYS fluent software needs to be determined. The domain is cuboid-shaped, with dimensions of 1000 mm at the front of the hydrofoil winglet, 1600 mm on the right and left sides of the hydrofoil winglet, 1000 mm on the top and bottom of the hydrofoil winglet, and 2000 mm at the back of the hydrofoil winglet, with a mesh size of 0.098 m (see Figure 7). The modelling parameters use k-Ω SST fluid models with a density of 1025 kg/m3 and boundary conditions consisting of inlet boundary conditions with a speed of 15.43 m/s and an outlet boundary condition with a pressure outlet. The modelling solution uses second-order discretization and an iterative process with standard Initialization.
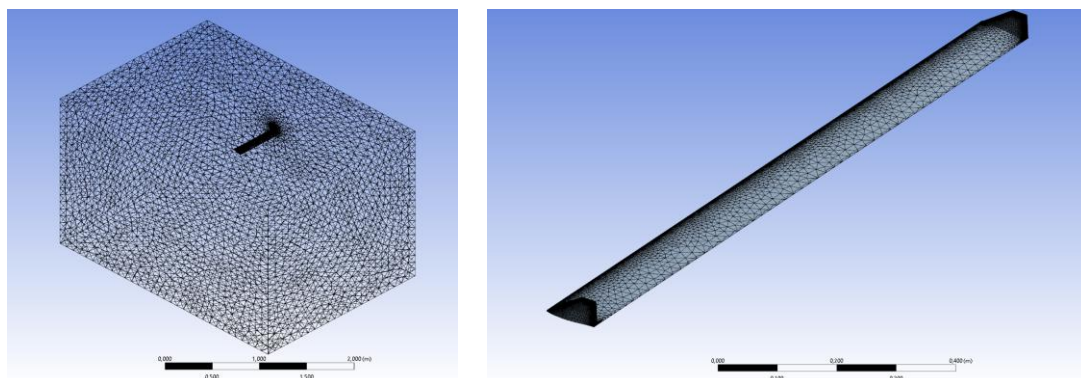

Fig. 7. Meshing of hydrofoil winglet

4. Results

4.1 Performance of Hydrofoil Winglet

The simulation results obtained using the Ansys Fluent software with 4 winglet variations and 8 speed variations obtain the results of lift and drag forces as shown in Figure 8 and 9, respectively.
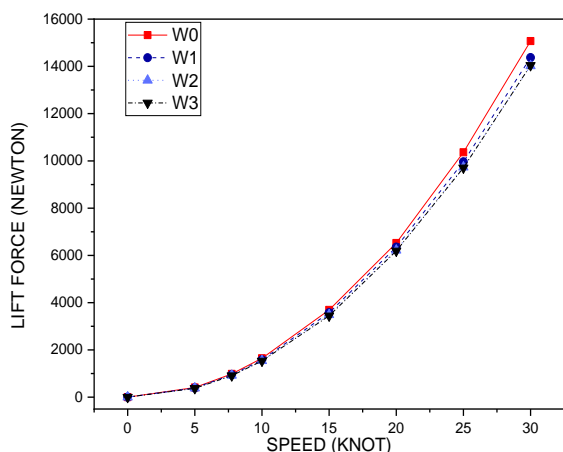

Fig.8. Lift force of hydrofoil winglets at speed variations
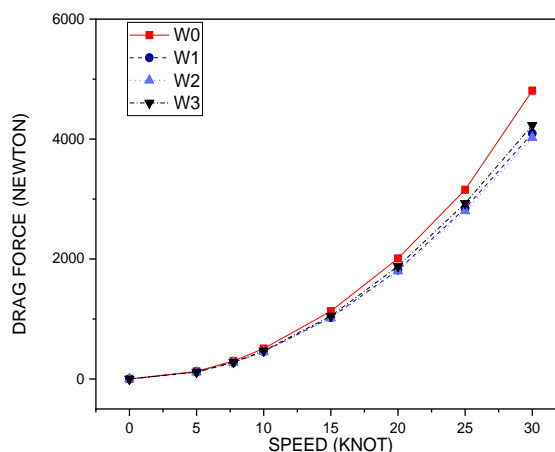

Fig.9. Drag force of hydrofoil winglets at speed variations

The figures informs that the W0 type has the largest amount of both lift and drag force in all speed variations. For instance, at a speed of 30 knots, it obtained 15069 Newton of lift force and 4808. Newton of drag force. However, it also shows the smallest L/D ratio, namely 3.13. In spite of generating a considerable force of lift, the drag force of W0 grows much bigger at higher speeds and dramatically reduces the L/D ratio. At the same speed, W1 generates 14369 Newtons of lift force and 4093 Newtons of drag force. It obtains the highest L/D ratio among the winglet variations, namely 3.51 (See Figure 10).

The high L/D ratio may increase the ship's efficiency since the significant lift force allows the ship to achieve lifting conditions more quickly. Simultaneously, the decreased drag force means that less engine power is required to achieve the design speed. As a result, when a hydrofoil has an optimal L/D ratio, it helps minimise fuel consumption since the design speed may be attained with less engine power.
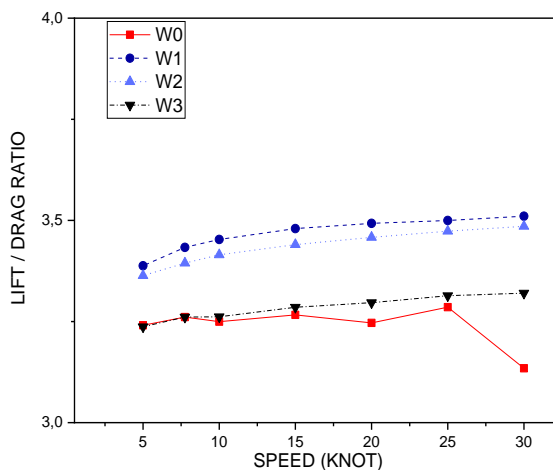

Fig.10. L/D ratio of hydrofoil winglets at speed varia

4.2 Flow Characteristics

In this study, data on velocity and pressure contours were collected to describe the fluid phenomena occur around the NACA 64(1)212 foil with W0-W3 winglet variations. Figure 11 below shows the pressure contours both in the suction and pressure sides.
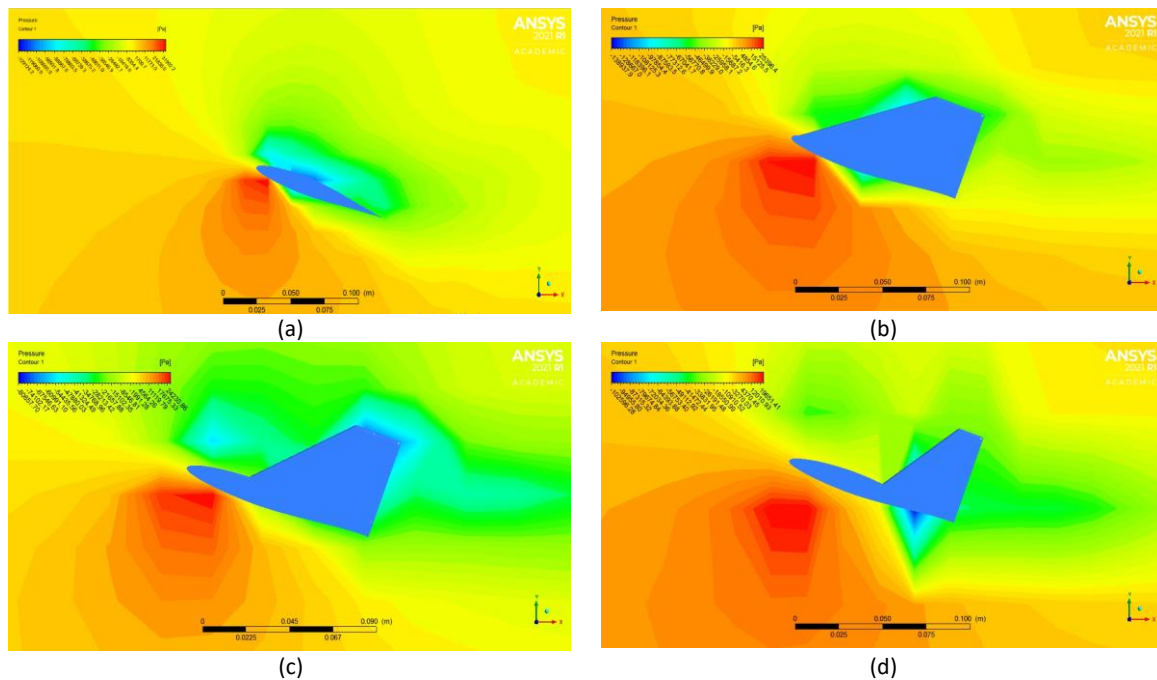

(a)

(b)

(c)

(d)

Fig. 11. Pressure Contour around winglets

Based on Figure 11, the pressure contours on the pressure sides of W0 and W1 hydrofoil winglets perform substantially larger forces than the other hydrofoil winglets. It mainly occurs near by the leading edge at approximately at 0.7 and 0.6 of the chord length measured from the maximum thickness for W0 and W1 respectively. In addition, the flow separation on W0 is obtained mainly on the maximum thickness of suction side, while on W3, it occurs mainly at the trailing edge. The low-pressure flow is also can be seen in the winglet tip of W1 and W2 (see Figure 11(b) and 11(c)). Low pressure caused by high-velocity flow increases the momentum of the boundary layer on the suction side, which means the minimum pressure gradient occurs on these winglet types. As a result, they are effective in preventing the flow from a high-pressure area to a lower-pressure one.
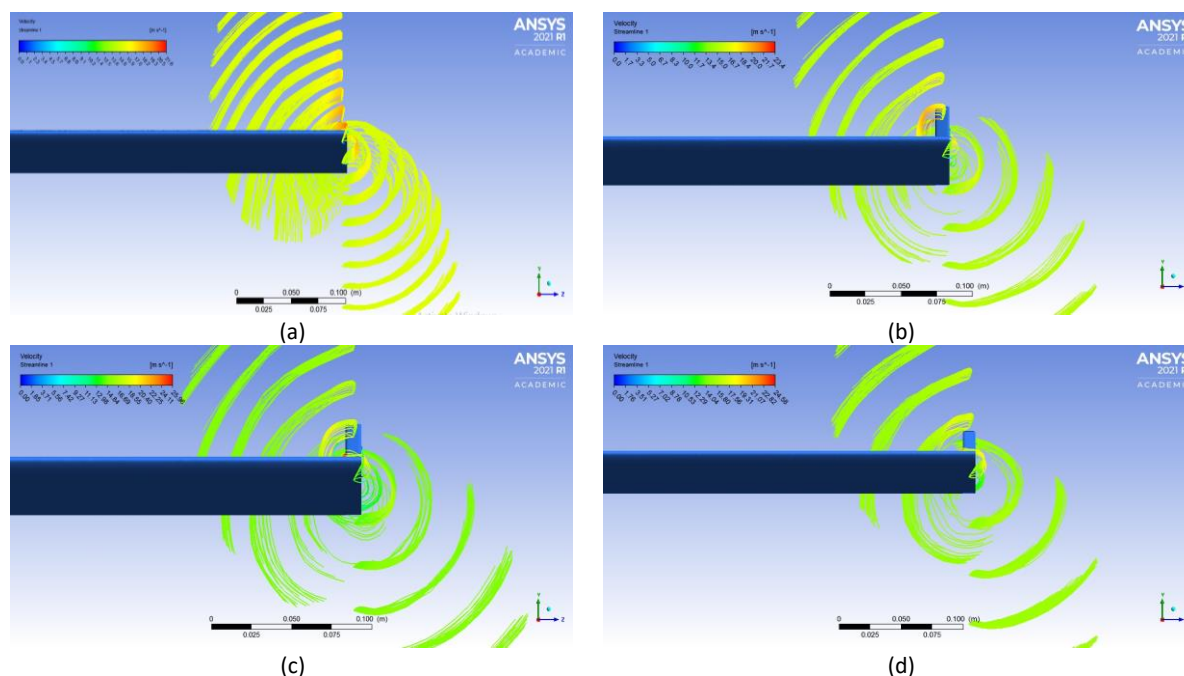
Fig.12. Flow Pattern around winglets

The flow velocity around the winglet can be seen in Figure 12 above. The fluid travelling from the pressure side to the suction side causes vortices at all winglets, which is known as the pressure gradient. The absence of winglets on the W0 type results in the greatest vortex compared to the other winglet forms. The W1 winglet (see Figure 12(b)) with the full CCR ratio, on the other hand, might diminish both the fluid flowing to the low-pressure side and the flow-induced vortex. When the drag force of the winglet is insignificant, including vortex-induced drag, as specified in the L/D ratio of the W1 winglet, it will aid the ship in attaining the design speed with the least amount of engine power. It implies that the hydrodynamic drag caused by the vortex that formed at the winglet would reduce fuel efficiency.

5. Conclusions

Among the studied hydrofoils, the winglet-less hydrofoil (W0) exhibits the most substantial lift force. However, its L/D ratio suffers due to notable drag. The absence of a winglet induces elevated pressure gradients, leading to vortex-induced drag. Conversely, the W1 model, featuring a fully enclosed root chord winglet, effectively manages flow on the pressure side, resulting in the highest L/D ratio. Importantly, winglets at the hydrofoil's ends mitigate vortex effects.

Acknowledgement

References

[1] Fitriadhy, A., N. Amira Adam, and M. Syafiq Zikry. "COMPUTATIONAL ANALYSIS ON HEAVE AND PITCH MOTIONS PERFORMANCE OF A HYDROFOIL SHIP." *Journal of Marine-Earth Science and Technology* 1, no. 1 (2020).

[2] Setiawan, Wira, Suardi Alamsyah, R. Jamal Ikhwani, and Luthfi Habibi. "Design of Hydrofoil Craft for Balikpapan-Penajam Route." (2020).

[3] Suryadi, Aji, Irfan Syarif Arief, and Amiadji Amiadji. "Analisa Pengaruh Sudut Serang Hidrofoil Terhadap Gaya Angkat Kapal Trimaran Hidrofoil." *Jurnal Teknik ITS* 5, no. 2 (2017).

[4]   Ni, Zao, Manhar Dhanak, and Tsung-chow Su. "Performance of a hydrofoil operating close to a free surface over a range of angles of attack." *International Journal of Naval Architecture and Ocean Engineering* 13 (2021): 1-11.

[5]   Azlin, M. An, CF Mat Taib, Salmiah Kasolang, and F. H. Muhammad. "CFD analysis of winglets at low subsonic flow." In *Proceedings of the World Congress on Engineering*, vol. 1, pp. 6-8. 2011.

[6]   Çetinkaya, Aras, and Uğur Oral Ünal. "A computational study into the effect of the winglets on the performance of fully submerged hydrofoils." *Applied Ocean Research* 104 (2020): 102357.

[7]   Mehta, Anshuman. "Different Types of Winglets and Their Corresponding Vortices Report 2." In *Bombay, Seminar at SMIT (June 2016)*. 2016.

[8]   Mouliswar, R. R., Karthik Chandrasekaran, Thiyagarajan Ranganathan, and Asokan Thondiyath. "Computational Fluid Dynamic Study on the Effect of Winglet Addition in Flapping Hydrofoils to Evaluate the Propulsive Performance of Wave Gliders." In *OCEANS 2022-Chennai*, pp. 1-4. IEEE, 2022.

[9]   Sun, Yueli, Jingjie Chen, Jincheng Cui, Qi Meng, and Ziheng Xing. "Comprehensive Analysis on the Contribution of Winglets Fuel Based on Contrast Experiment." In *2017 International Conference on Applied Mathematics, Modelling and Statistics Application (AMMSA 2017)*, pp. 256-260. Atlantis Press, 2017.

[10]   Guerrero, Joel, Marco Sanguineti, and Kevin Wittkowski. "CFD study of the impact of variable cant angle winglets on total drag reduction." *Aerospace* 5, no. 4 (2018): 126.

[11]   Kazim, Ali Hussain, Abdullah Hamid Malik, Hammad Ali, Muhammad Usman Raza, Awais Ahmad Khan, Tauseef Aized, and Aqsa Shabbir. "CFD analysis of variable geometric angle winglets." *Aircraft Engineering and Aerospace Technology* 94, no. 2 (2022): 289-301.

[12]   Putnam, Neola, Gregory Dickert, and Caleb Wagner. "On the design, construction, and testing of a fully-submerged canard hydrofoil system for a low-speed solar boat." *International Hydrofoil Society* (2014).

[13]   Maeda, S., T. Sano, M. Iino, M. Farhat, and A. Amini. "Effect of the winglet on reduction of blade tip vortex from elliptical hydrofoil." In *IOP Conference Series: Earth and Environmental Science*, vol. 774, no. 1, p. 012054. IOP Publishing, 2021.

[14]   Amini, Ali, Martino Reclari, Takeshi Sano, Masamichi Iino, and Mohamed Farhat. "Suppressing tip vortex cavitation by winglets." *Experiments in Fluids* 60 (2019): 1-15.

[15]   Leishman, J. Gordon. "Introduction to Aerospace Flight Vehicles." (2022).